Behavior of Raman modes in InPBi alloys under hydrostatic pressure

Behavior of Raman modes in InPBi alloys under hydrostatic pressure

Cite as: AIP Advances **9**, 035120 (2019); https://doi.org/10.1063/1.5085132
Submitted: 09 December 2018 . Accepted: 01 March 2019 . Published Online: 13 March 2019

Changcheng Zheng, Xiaohu Wang, Jiqiang Ning, Kun Ding, Baoquan Sun, Shumin Wang, and Shijie Xu

Behavior of Raman modes in InPBi alloys under hydrostatic pressure

Cite as: AIP Advances 9, 035120 (2019); doi: 10.1063/1.5085132
Submitted: 9 December 2018 • Accepted: 1 March 2019 •
Published Online: 13 March 2019

Changcheng Zheng,[1,2,a)] Xiaohu Wang,[3] Jiqiang Ning,[4,a)] Kun Ding,[5] Baoquan Sun,[5] Shumin Wang,[2,6] and Shijie Xu[7]

AFFILIATIONS

[1]Physics Division, Department of Mathematical Sciences, Xi'an Jiaotong-Liverpool University, Suzhou 215123, China
[2]Key Laboratory of Terahertz Solid-State Technology, CAS, Shanghai Institute of Microsystem and Information Technology, Chinese Academy of Sciences, 865 Changning Road, Shanghai 200050, China
[3]Institute of Microelectronics, Tsinghua University, Beijing 100084, China
[4]Vacuum Interconnected Nanotech Workstation, Suzhou Institute of Nano-Tech and Nano-Bionics, Chinese Academy of Sciences, Suzhou 215123, China
[5]State Key Laboratory of Superlattices and Microstructures, Institute of Semiconductors, Chinese Academy of Sciences, Beijing 100083, China
[6]Department of Microtechnology and Nanoscience, Chalmers University of Technology, 41296 Gothenburg, Sweden
[7]Department of Physics, The University of Hong Kong, Pokfulam, Hong Kong, China

[a)]**Authors to whom correspondence should be addressed:** changcheng.zheng@xjtlu.edu.cn and jqing2015@sinano.ac.cn.

ABSTRACT

Raman spectra of InPBi alloys with bismuth amount 0.3%-2.0% were measured under hydrostatic pressure in diamond anvil cell up to ~4 GPa at room temperature. Two bismuth related Raman modes were identified and their evolutions under pressure were studied. The linear pressure coefficients of these two modes are determined to be 1.292 and 2.169 cm^{-1}/GPa, respectively. The different behaviors of these two modes under pressure suggest that they may have distinct origins. InP related Raman modes were also investigated including two InP related modes caused by Bi doping.

INTRODUCTION

As a typical III-V narrow band gap semiconductor material, InP has various applications in infrared optoelectric devices. By doping with Bi, InPBi alloys could be formed and it was predicted to be one of the most stable candidates in fabricating infrared optoelectric devices.[1] Recently, high quality InPBi alloys were successfully synthesized by gas source molecular beam epitaxy (MBE) method at low temperature.[2] The high crystal quality of $InP_{1-x}Bi_x$ has been confirmed by X-ray diffraction and Rutherford Backscattering Spectrometry (RBS) measurements.[2,3] It is very important to build up a full understanding of the physical properties of this kind of material in order to realize all its potential applications. Since optical means are powerful and nondestructive ways for investigating material properties, photoluminescence and Raman spectra are used to study the emission bands and vibration modes in $InP_{1-x}Bi_x$, respectively.[2–6] It was found out that incorporation of Bi inside InP substrate would reduce its band gap which made it more suitable for applications in near infrared region.[2,3,5] At the meantime, Bi doping also caused additional Raman vibration modes compared with InP layer grown at the same temperature on InP substrate.[4,6] Two new bismuth related modes were identified at ~150 and ~170 cm^{-1}, and were attributed to InBi vibration modes.[4,6] Furthermore, compared with InP layer, two more InP related Raman modes at ~312 and ~337 cm^{-1} were also observed,[4,6] possibly caused by lattice distortion in InP due to Bi doping. Although these additional modes were discussed in recent reports,[4,6] here we would like to provide further evidence for identifying these modes from Raman spectra under hydrostatic pressure.

Evolution of optical properties, especially photoluminescence (PL) and Raman spectra, of semiconductors and nanostructures under pressure provides important information for investigating their band structure, lattice vibration nature, etc.[7–10] The linear pressure coefficients of LO and TO phonon modes from InP were derived as 5.6 and 6.3 cm^{-1}/GPa, respectively.[7] In this letter, we report the first experimental Raman study of InPBi alloys under hydrostatic pressure (up to ~4 GPa). Both Bi and InP Raman modes are analyzed against pressure. Features including peak position, full-width at half maximum (FWHM), integrated peak intensity are investigated.

EXPERIMENTAL

InPBi layer with thickness ~420 μm was grown on InP substrate at ~320 °C by V90 gas source molecular beam epitaxy (MBE).[2] Elementary Bi source was used and its flux was controlled by adjusting cell temperature. Bi incorporation in InP layers was estimated from RBS measurements. More details about the growth process can be found in Ref. 2. In this work, InPBi alloys with Bi concentrations of 0.3%, 1.0%, 2.0% were studied (named as InPBi_1, InPBi_2, and InPBi_3, respectively) with comparison from a InP layer (named as InP LT) grown under similar conditions. Room temperature Raman spectra were taken under the back-scattering geometry by a confocal micro-Raman system (LabRAM HR Evolution system) with 514.5 nm excitation from a Ar^+ laser. For measurements under pressure, the sample was thinned into tens of micrometers mechanically from the substrate, and then loaded into the diamond anvil cell (DAC). Condensed argon was introduced as the pressure-transmitting medium in the DAC. PL peaks from Ruby powders were used for calibrating the pressure value in the DAC.

RESULTS AND DISCUSSION

Figure 1 shows the Raman spectra of these four samples in ambient environment at room temperature. Two InP vibration peaks at 306.46 and 343.20 cm^{-1} are observed from undoped InP layer, which are attributed to InP TO(Γ) and LO(Γ),[4,7] respectively (denoted as InP TO-1 and InP LO-2). All peak features, such as peak position, FWHM and integrated peak intensity, are obtained by fitting the Raman spectrum with Lorentz functions. The low energy shoulder of the InP TO-1 peak was attributed to the lower branch of the coupled plasmon-LO mode.[4] These two Raman peaks are also observed from three InPBi samples. Additionally, two Bi related Raman peaks are identified at ~150 and ~170 cm^{-1} (denoted as Bi-1 and Bi-2, respectively), together with two more InP related Raman modes at ~312 and ~337 cm^{-1} (denoted as InP TO-2 and InP LO-1, respectively) in InPBi samples. The peak positions of these two newly emerged InP related vibration modes in InPBi samples are very close to 313 cm^{-1} (TO(L)) and 336 cm^{-1} (LO(X)) modes from InP.[7] This is probably caused by the lattice distortion in InP due to Bi doping. The lattice distortion in InP will lead to an effective polarizability derivative for the TO(L) and LO(X) modes, which results in the previously inactive modes being detected. This effect is reversed to a certain degree under external hydrostatic pressure which will be discussed later.

To develop a deeper understanding of these observed vibration modes, Raman spectra of InPBi alloys under hydrostatic

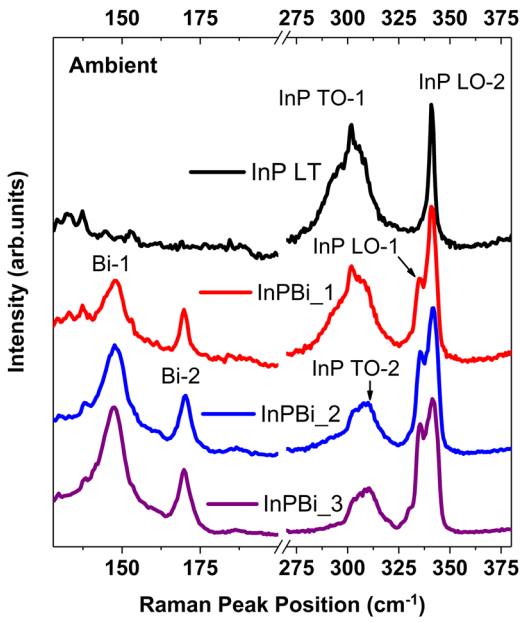

FIG. 1. Raman spectra of InP layer and InPBi alloys with Bi concentrations 0.3%, 1.0% and 2.0%, respectively, in ambient environment.

pressure were measured. Generally, Raman signal from samples in DAC are much weaker than those in ambient environment due to the scattering in pressure transmission medium (condensed

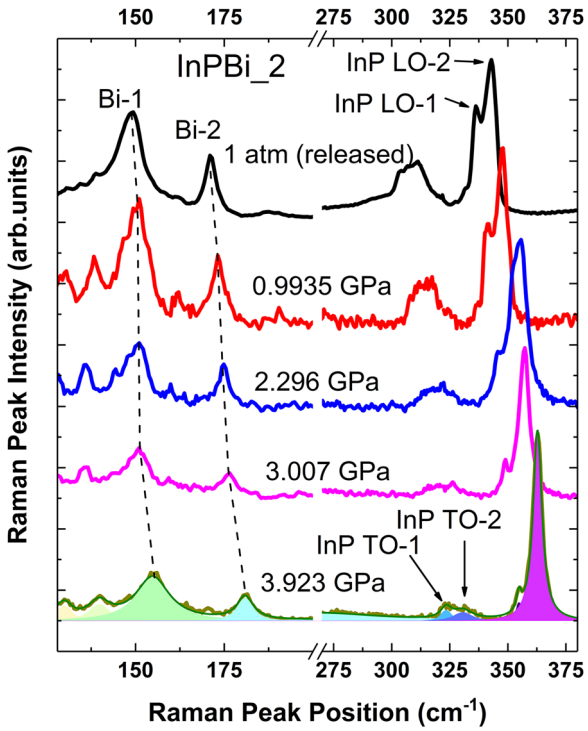

FIG. 2. Raman spectra of InPBi_2 under hydrostatic pressure in DAC, up to ~4 GPa.

argon in our experiments) and the diamond window and also the decrease in collection efficiency for using a long focus range objective lens. Signals from InPBi_1 and InPBi_2 were obtained successfully in DAC, although the two Bi related modes were hard to distinguish from InPBi_1 sample. Here the Raman spectra from InPBi_2 in DAC under various pressures are depicted in Fig. 2. We should mention that after careful analysis, the InP related Raman peaks demonstrate the same behavior under pressure based on observations from InPBi_1 and InPBi_2. Pressure value inside the DAC was calibrated by the peak position of Ruby PL R1 line based on the empirical formula developed from Murnaghan equation,[11–13]

$$P = \frac{1904}{B}\left[\left(\frac{\lambda}{\lambda_0}\right)^B - 1\right]$$

where P is the pressure in GPa, λ_0 the peak position of Ruby R1 line at ambient pressure, λ the peak position of Ruby R1 line at certain pressure (λ_0 and λ values were obtained by fitting the Ruby R1 emissions with Lorentz function), and B is a constant of 7.665.

Figure 2 shows the Raman spectra of InPBi_2 under various hydrostatic pressures. The same data process was performed. As expected, all Raman modes demonstrate a blue-shift as environmental pressure increases. Additionally, the ratio of peak intensity of InP LO-1 to that of InP LO-2 decreases when the pressure goes up. As mentioned earlier, the InP LO-1 Raman mode is probably induced by lattice distortion of InP caused by Bi doping. The application of an external hydrostatic pressure can effectively reduce the distortion of the InP lattice, which therefore weakens the polarizability derivatives and suppresses the doping-induced mode, leading to the intensity drop of the InP LO-1 peak, while the InP LO-2 Raman mode is less affected. Based on the fitting results, the Raman peak positions versus pressures of different modes are summarized in Fig. 3. A linear fitting was performed for the data in Fig. 3 for each Raman vibration mode and the linear pressure coefficients are listed in Table I.

For the two InP related Raman vibration modes observed in InP layer and also all other samples, InP TO-1 and InP LO-2, their linear pressure coefficients are found to be 4.404 and 5.377 cm^{-1} GPa^{-1}, respectively. The two coefficients are close to those reported experimental values,[8,9] and also comparable to theoretical calculations.[10] It should be noted that a parabolic function was used for obtaining the pressure coefficients, although the second order coefficient was very small.[9] Interestingly, two newly emerged InP related

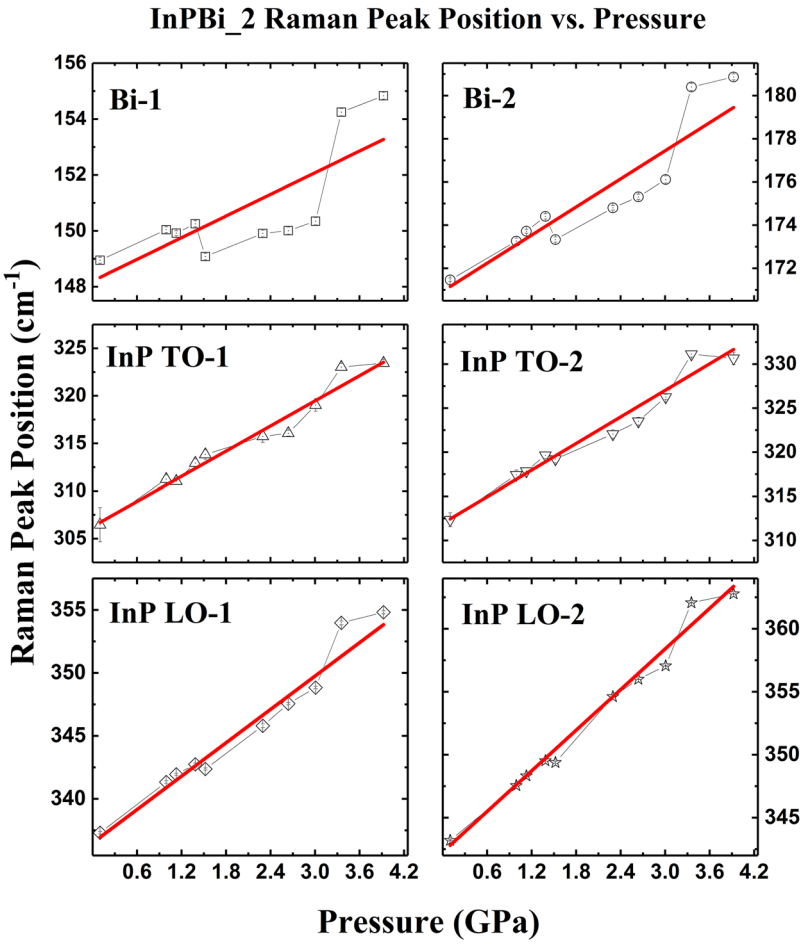

FIG. 3. Peak positions of various Raman vibration modes in InPBi measured from InPBi_2 in DAC at different hydrostatic pressures. Red lines are the linear fitting results, respectively.

TABLE I. Linear pressure coefficients of various Raman vibration modes in InPBi obtained by fitting data in Fig. 3.

	Bi-1	Bi-2	InP TO-1	InP TO-2	InP LO-1	InP LO-2
Pressure coefficient (cm^{-1}/GPa)	1.292 ± 0.344	2.169 ± 0.291	4.404 ± 0.398	5.030 ± 0.441	4.418 ± 0.281	5.377 ± 0.419
Calculated values (cm^{-1}/GPa) [10]			4.95		4.71	

modes caused by incorporation of Bi atoms, InP TO-2 and InP LO-1, demonstrate different behavior compared with these of InP TO-1 and InP LO-2, respectively. This may partially show the dispersion relations of TO and LO phonons in InP.[14] Further experiments, such as polarization dependent Raman spectrum, will be carried out to investigate this.

As for two Bi related Raman modes, their linear pressure coefficients are much smaller than those of the InP related modes, and also smaller than those calculated values of typical LO and TO phonon modes of other III-V semiconductors.[10] Although, the pressure coefficients of phonons in InBi were not calculated in that work probably because of the difficulty in calculation regarding to the heavy atomic mass of Bismuth, we would like to tentatively assign the observed Bi related Raman modes, Bi-1 and Bi-2, to α-Bi_2O_3 A_g Raman mode and overtone of Bi cluster Raman mode, respectively, rather than InBi related Raman modes. The Bi_2O_3 A_g Raman mode was observed from Bi_2O_3 powder or crystals at 151~153 cm^{-1},[15–17] and its linear pressure coefficient was found to be around 2 $cm^{-1}GPa^{-1}$ from experiments and also theoretical simulation.[15,17] In our study, the Bi-1 Raman mode is at ~150 cm^{-1} in ambient and its linear pressure coefficient is found to be ~1.3 $cm^{-1}GPa^{-1}$ (with noticeable fitting errors because of the weak Raman signal). Bi_2O_3 may form due to the exposure of sample to air in the sample handling and storage process, or the laser oxidation caused in the optical testing experiments performed in ambient conditions.[16] On the other hand, first-order Raman modes were observed from bismuth at 70 and 97 cm^{-1}, which were assigned to Bi E_g and A_{1g} modes, respectively.[16,18] The Bi-2 Raman mode observed in this work, at ~170 cm^{-1}, is probably from the overtone of these two Bi Raman modes. The obtained linear pressure coefficient of Bi-2 mode, ~2.2 $cm^{-1}GPa^{-1}$ is comparable to the reported values for overtone modes from Bi (3~4 $cm^{-1}GPa^{-1}$).[18] Furthermore, the FWHM of Bi-1 and Bi-2 Raman modes tend to increase with pressure while that of InP Raman modes show a decrease tendency (results not shown here). This also suggests that the two Bi related Raman modes may not come from InBi vibrations. Investigating the vibrational modes in the Raman spectra under hydrostatic pressure helps to identify whether and how foreign atoms are embedded in the hosting material and how the host lattice is distorted accordingly. The obtained information can also be used to further manipulate the physical properties of both the host and the doped atoms, by adopting different doping methods.

CONCLUSION

To summarize, based on Raman spectrum measurements of InPBi alloys under hydrostatic pressure, linear pressure coefficients of various Raman modes are obtained by fitting experimental results. The two Bi related Raman modes (~150 and ~170 cm^{-1}) are identified and tentatively assigned to α-Bi_2O_3 A_g Raman mode and overtone of Bi cluster Raman mode, respectively. InP LO and TO phonon mode behaviors under pressure are also observed and discussed. Investigation of these Raman modes in doped InP is certainly helpful for understanding the nature of impurity incorporations in it and also provides useful information for realizing its potential applications.

ACKNOWLEDGMENTS

CCZ acknowledges financial support from an open project from State Key Laboratory of Functional Materials for Informatics, Shanghai Institute of Microsystem and Information Technology, and partial support from Natural Science Foundation of China (No.: 11504299). JQN acknowledges the financial support from Natural Science Foundation of China (11874390) and Hundred Talents Program of Chinese Academy of Sciences.

REFERENCES

[1] M. A. Berding, A. Sher, A. B. Chen, and W. E. Miller, J. Appl. Phys. **63**(1), 107–115 (1988).
[2] K. Wang, Y. Gu, H. F. Zhou, L. Y. Zhang, C. Z. Kang, M. J. Wu, W. W. Pan, P. F. Lu, Q. Gong, and S. M. Wang, Sci. Rep. **4**, 5449 (2014).
[3] Y. Gu, K. Wang, H. F. Zhou, Y. Y. Li, C. F. Cao, L. Y. Zhang, Y. G. Zhang, Q. Gong, and S. M. Wang, Nanoscale Res. Lett. **9**, 24 (2014).
[4] W. W. Pan, J. A. Steele, P. Wang, K. Wang, Y. X. Song, L. Yue, X. Y. Wu, H. Xu, Z. P. Zhang, S. J. Xu, P. F. Lu, L. Y. Wu, Q. Gong, and S. M. Wang, Semicond. Sci. Tech. **30**(9), 094003 (2015).
[5] P. Wang, W. W. Pan, C. F. Cao, X. Y. Wu, S. M. Wang, and Q. Gong, Jpn. J. Appl. Phys. **55**(11), 115503 (2016).
[6] G. N. Wei, Q. H. Tan, X. Dai, Q. Feng, W. G. Luo, Y. Sheng, K. Wang, W. W. Pan, L. Y. Zhang, S. M. Wang, and K. Y. Wang, Chinese Phys. B **25**(6), 066301 (2016).
[7] B. Ulrici and E. Jahne, Phys. Status Solidi B **74**(2), 601–607 (1976).
[8] M. F. Whitaker, S. J. Webb, and D. J. Dunstan, J. Phys.: Condens. Mat. **10**(38), 8611–8618 (1998).
[9] R. Trommer, H. Muller, M. Cardona, and P. Vogl, Phys. Rev. B **21**(10), 4869–4878 (1980).
[10] S. Q. Wang and H. Q. Ye, J. Phys.: Condens. Mat. **17**(28), 4475–4488 (2005).
[11] F. D. Murnaghan, PNAS **30**, 244–247 (1944).
[12] H. K. Mao and P. M. Bell, Science **200**(4346), 1145–1147 (1978).
[13] X. M. Dou, K. Ding, D. S. Jiang, X. F. Fan, and B. Q. Sun, ACS Nano **10**(1), 1619–1624 (2016).
[14] P. H. Borcherds, G. F. Alfrey, D. H. Saunderson, and A. D. B. Woods, J. Phys. C: Solid State **8**(13), 2022–2030 (1975).
[15] C. Chouinard and S. Desgreniers, Solid State Commun. **113**(3), 125–129 (1999).
[16] K. Trentelman, J. Raman Spectrosc. **40**(5), 585–589 (2009).
[17] A. L. J. Pereira, O. Gomis, J. A. Sans, J. Pellicer-Porres, F. J. Manjon, A. Beltran, P. Rodriguez-Hernandez, and A. Munoz, J. Phys.: Condens. Mat. **26**(22), 225401 (2014).
[18] H. Olijnyk, S. Nakano, and K. Takemura, Phys. Status Solidi B **244**(10), 3572–3582 (2007).